

Remote electrical arc suppression by laser filamentation

Elise Schubert¹, Denis Mongin¹, Jérôme Kasparian^{2,*} and Jean-Pierre Wolf¹

¹*GAP-Biophotonics, Université de Genève,
Chemin de Pinchat 22, 1211 Genève 4, Switzerland and*

²*GAP-Biophotonics, Université de Genève,
Chemin de Pinchat 22, 1211 Genève 4, Switzerland*

(Dated: August 28, 2018)

Abstract

We investigate the interaction of narrow plasma channels formed in the filamentation of ultrashort laser pulses, with a DC high voltage. The laser filaments prevent electrical arcs by triggering corona that neutralize the high-voltage electrodes. This phenomenon, that relies on the electric field modulation and free electron release around the filament, opens new prospects to lightning and over-voltage mitigation.

* jerome.kasparian@unige.ch

I. INTRODUCTION

Since the pioneering work of Benjamin Franklin [1], both the mechanisms of lightning and lightning protection have entered in the area of science. Lightning occurs after vertical winds, with speeds up to 20 m/s, separate charges within thunderclouds. The resulting static electric fields reach 10 – 15 kV/m at ground level, and up to 50 kV/m some hundreds of meters above ground. These high fields initiate corona discharges, that under sufficient electric field and charge supply develop into streamers, and then ionized plasma channels, or leaders. The latter give rise to a lightning strike if they connect regions of clouds and/or of the ground with opposite charges [2].

Lightning protection of buildings or other facilities is mainly focused on capturing the lightning strikes and safely conducting their energy to the earth, via a grounding conductor. Alternatively, it has been proposed to use lasers to divert lightning to harmless places by guiding it using the ionized path generated by laser pulses [3, 5–13, 36]. Laser filaments have also been used as a probe to investigate the dynamics of high-voltage discharges [14, 15] and leaders [16–18].

Laser filamentation [19–21] is a self-guided propagation regime of high power, ultrashort pulses. It relies on an interplay between the self-focusing Kerr effect and a defocusing effect caused by ionization of the medium, as well as higher-order Kerr effects [22–25]. The resulting dynamic balance clamps the filament intensity to 5×10^{13} W/cm³ [26, 27] over a typical diameter of 100 μ m, producing a continuously ionized plasma channel.

Most of the work on laser triggering of high-voltage discharges to date uses high-voltage pulses synchronized with the laser, unlike the quasi-DC field typical of thunderclouds. Furthermore, triggering lightning ultimately implies collecting the discharge by means of a classical lightning rod, with an adequate design and/or location to avoid indirect effects of lightning, i.e., electromagnetic perturbation, in the vicinity of the impact location.

In contrast, preventing breakdown at all by remotely unloading thunderclouds may offer a more efficient protection. In that regard, grounded wires of 100 μ m or less have been shown to inhibit electrical arcs by initiating a streamer-free corona (or ultra-corona) [28]. Visible with naked eye as a glow discharge, ultra-corona disperses a space charge that stops sparking. Here, we show that laser filaments can induce a similar process and neutralize DC high-voltage electrodes while preventing electrical arcs, even remotely.

II. EXPERIMENTAL SETUP

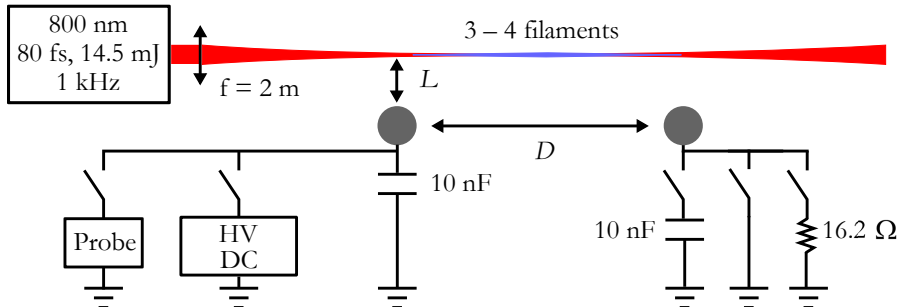


Figure 1: Experimental setup. A Ti:Sapphire laser focused with an $f = 2$ m lens creates 3–4 ~ 20 cm long filaments. The electrode with a capacitor is charged to 14 kV and the generator is then disconnected. After the laser has been shined, the residual voltage on the electrode is measured via a HV-probe. The distance between the electrodes and the distance from the electrodes to the filament can be changed.

The experimental setup (Figure 1) relied on a DC high-voltage generator (100 kV, 200 μ A maximum current, or 14 kV, 7 mA with a 10 nF capacitor attached to store charge and allow the delivery of stronger currents), connected to spherical electrodes (diameter 1.2 cm) that could be placed arbitrarily on either side of the laser beam, at various axial and longitudinal positions. Unless otherwise specified, one electrode was grounded, while the other one was set to the potential of the high-voltage generator. Also, the generator could be disconnected from the capacitor and the electrode, so as to investigate the flow of a fixed charge Q between the electrodes and the associated unloading of the capacitor.

A Ti:Sapphire chirped pulse amplification system delivered 80 fs pulses of 14.5 mJ centered at 800 nm at a 1 kHz repetition rate, unless otherwise specified. This beam of initial diameter 4 cm was slightly focused ($f = 2$ m), generating 3 to 4 self-guided filaments. Due to the external focusing of the beam, the filament length was about 20 cm in our configuration. As detailed in the next section, the beam was sent in various configurations relative to the electrodes, from a close vicinity of 2 mm (the minimum distance to avoid the edge of the beam to ablate matter from the electrodes) to 30 cm distance.

The current flowing through the ground electrode was measured by monitoring the voltage on a 16.2 Ω resistor connecting the latter to the earthing. The signal was recorded

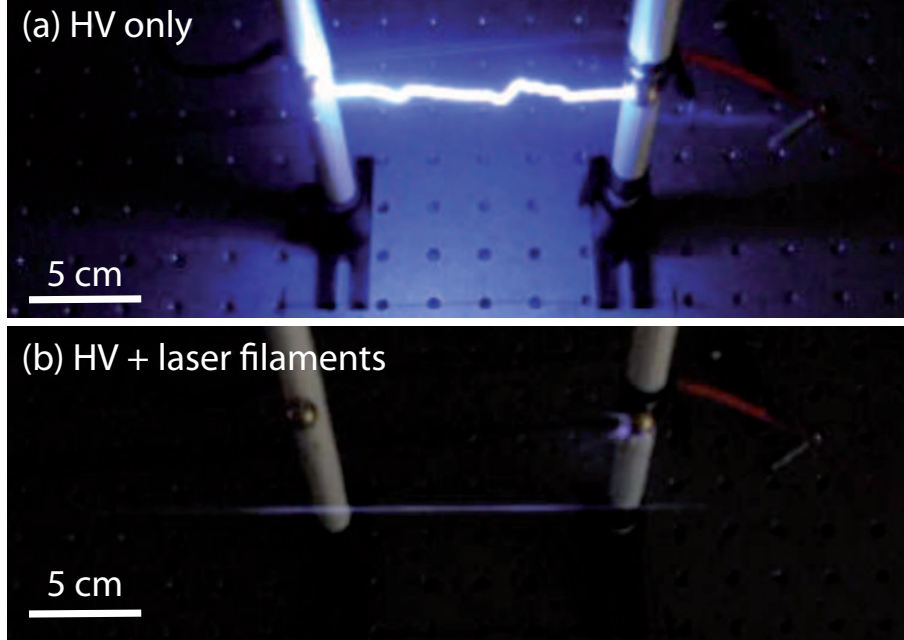


Figure 2: Electrical arc suppression by laser-induced neutralization under 100 kV (a) Electrical arc without laser (b) Arc inhibition when the laser is turned on.

on a 100 MHz bandwidth oscilloscope, synchronized with the laser pulses by a photodiode detecting the scattering of the beam on the beam dump, 2.2 m downstream of the interaction region. The discharge of the capacitor attached to the high-voltage electrode was characterized using a high-voltage probe (Fluke 80K-40 HV probe).

The experiments have been performed at room temperature ($T = 20^\circ\text{C}$), at a relative humidity around 30%. Correspondingly, the background resistivity of the air is about $3 \times 10^{14} \Omega \cdot \text{m}$ [29].

III. RESULTS

A. Electrical arc suppression

Figure 2 and the Supplementary movie clearly illustrate electrical arc suppression by laser filaments. Applying 100 kV (Figure 2(a)) in a 12 cm gap between the electrodes, a value close to the threshold for spark discharges, results in typically one electrical arc per second. Switching on the laser in the vicinity of the electrodes immediately suppresses the sparking (Figure 2(b)). Instead, a glow discharge connects the electrodes to the filament, even if the

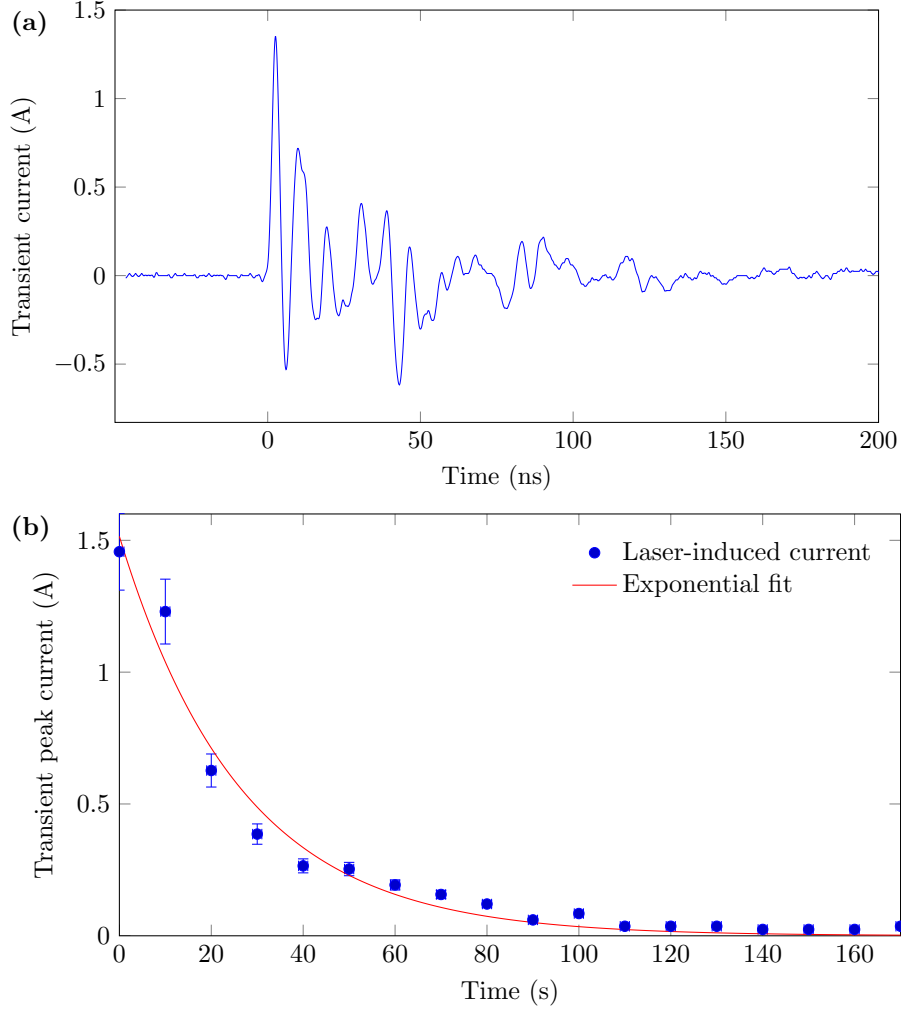


Figure 3: Laser unloading of a 10 nF capacitor at +14 kV. The electrodes were placed at a distance $D = 16 \pm 0.2$ cm apart, at a lateral distance L of 2 mm from the laser beam.

(a) Laser-induced current. Time 0 corresponds to the laser pulse. (b) Decay of the magnitude of the peak current, corresponding to the capacitor discharge.

latter is several centimeters away from the electrodes. Furthermore, the blueish glow of the filament, that is typical of the laser-generated plasma [20, 21], is much brighter in presence of the high-voltage than without it evidencing increased avalanche ionization in the filament under the electric field.

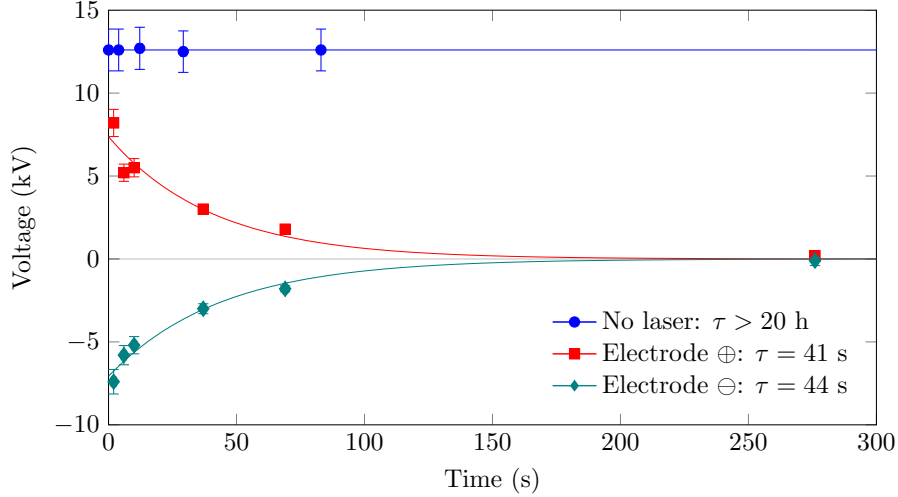


Figure 4: Simultaneous discharge of capacitors loaded under ± 14 kV, with a 16 cm gap between the electrodes, placed at $L = 2$ mm from the laser. The lines display exponential fits, τ being the decay time.

B. Spark-free neutralization

To better understand the electrical arc suppression and the associated glow discharge, we investigated the current flow induced by the laser filaments between the two electrodes with a 10 nF capacitor on the HV side, loaded under +14 kV. Without the laser, no measurable current flows between the electrodes, so that the capacitor keeps its load without measurable leak for over 20 hours. In contrast, each laser pulse results in a current burst (Figure 3(a)). The time delay between the laser pulse and the initiation of the corresponding current burst is shorter than the 5 ns time resolution of our detection system. It is therefore faster than the time required to establish a negative corona discharge, that lies in the 100 ns range [14].

These bursts progressively unload the capacitor (Figure 3(b)), with a decay time $\tau = 25$ s, corresponding to 25000 laser pulses. The laser-induced current is still observed when the laser is shifted laterally up to $L = 30$ cm away from the electrodes.

We characterized the flow of charges from one electrode to the other by attaching an initially empty capacitor C_2 to the ground electrode (see Figure 1). Under laser influence, the high-voltage capacitor C_1 progressively discharges. About one third of the charge from C_1 indeed reaches C_2 . As a result the charge of the latter reaches a maximum after 81 s, before decaying again.

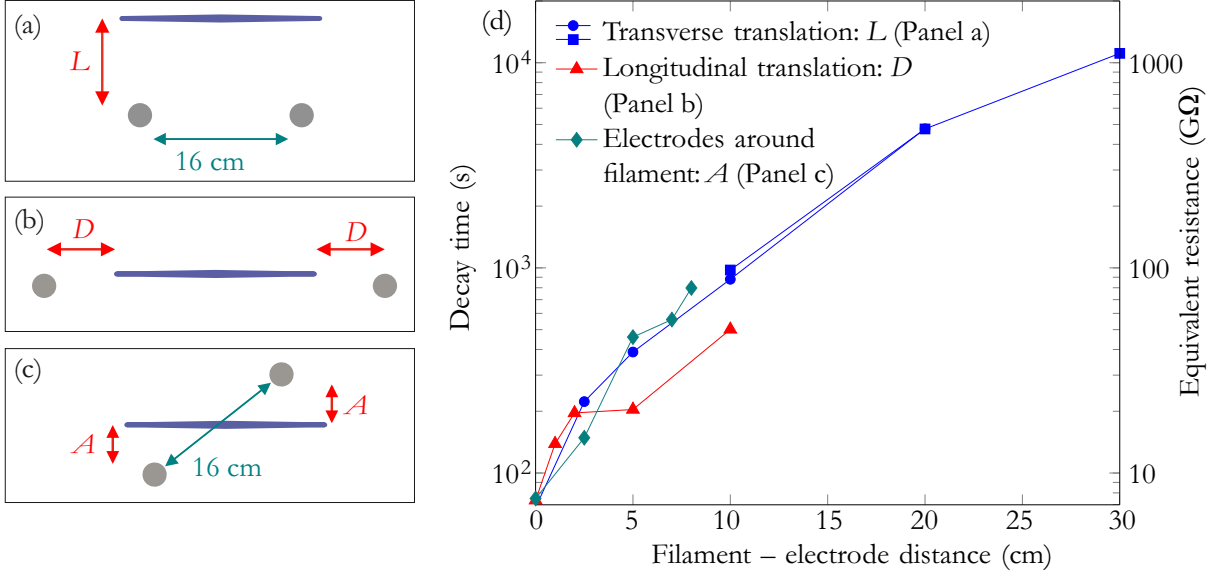


Figure 5: Effect of geometry on laser-induced neutralization. (a-c) Geometrical configurations: (a) transverse and (b) longitudinal distances, and (c) filament crossing the electrode gap. The gray circles represent the electrodes, and the blue line is the filament. (d) Decay time of the charge as a function of the distance between the electrodes and the filaments.

In contrast, when both 10 nF capacitors are simultaneously pre-loaded under +14 and -14 kV, respectively, in a floating configuration, they unload symmetrically (Figure 4), independently from the electrode polarity.

C. Geometrical considerations

Associated with electrical arc inhibition, the laser filaments can thus induce current and consequently neutralize the high-voltage even remotely. More precisely, we investigated three geometrical configurations. In the first one, the laser beam was moved away laterally from the electrodes and parallel to the gap (Figure 5(a)). In the second one, the electrodes were taken apart from one another, beyond the filament ends: the filament-distances therefore increased longitudinally (Figure 5(b)). Finally, we rotated the electrodes on a 16 cm axis centered around the filament. Tilting the axis varied the filament–electrode distance (Figure 5(c)).

In these three configurations, the decay times (Figure 5(d)) are similar for identical

distances between the electrodes and the filament. Therefore, the distance between the filament and the electrodes, rather than the geometrical configuration, governs the laser-induced neutralization. In particular, setting the filament parallel or perpendicular to the electrode gap results in similar laser-induced neutralization times.

Furthermore, the decay time of the charge $Q_0 = C \cdot V = 1.4 \times 10^{-4}$ C increases with the filament–electrode distance, from 68 s at 0.2 cm, to 3.1 h at 30 cm. This increase is linear up to a typical filament–electrode distance of 10 cm. Beyond this distance, the decay time tends to grow quadratically with increasing filament–electrode distances, while the decay of the charge progressively deviates from exponential, suggesting the occurrence of a new regime at long distances. However, even for a filament–electrode distance of 30 cm equal to twice the gap between the electrodes, the laser accelerates the unloading of the setup by one order of magnitude, illustrating the long-range effect of the laser filaments.

The exponential decay of the charge, together with its linear dependence with distance at least over the first 10 cm, are consistent with the simple picture of the discharge of an RC circuit. Within this rough, quasi-stationary description, the observed decay times correspond to effective resistances of $6.8 \text{ G}\Omega$ to $1 \text{ T}\Omega$, since $C = 10 \text{ nF}$, as displayed on the right vertical axis of Figure 5. Note that, to keep reasonable experimental times, the measurement at 30 cm has been performed with a capacitor reduced to 200 pF, and then renormalized to $C = 10 \text{ nF}$. We checked for 10 and 20 cm distances that this procedure yields consistent results (blue squares in Figure 5(d)).

Still, for a given filament–electrode distance, the charge decays slightly faster when the beam passes close to the electrodes and the filament bridges part of the electrode gap (Figure 5(b)), as compared to the other configurations. This may be due to the longitudinal plasma density along the filament, that rises faster at the beginning of the filament than it falls down at its end [20, 21]. As a consequence, the ends of the ionized region cannot be precisely defined.

As a result of the longitudinal electron density profile asymmetry in the filament, the charge decays 6.5 times faster when the high-voltage electrode is located 20 cm before the filament than at the same distance beyond it (Figure 6). This strongly asymmetric behavior illustrates the key role played by the high density of free charges released in the laser filament. In contrast, the neutralization is insensitive to the position of the grounded electrode, as well as to the longitudinal position of the electrodes within the filament.

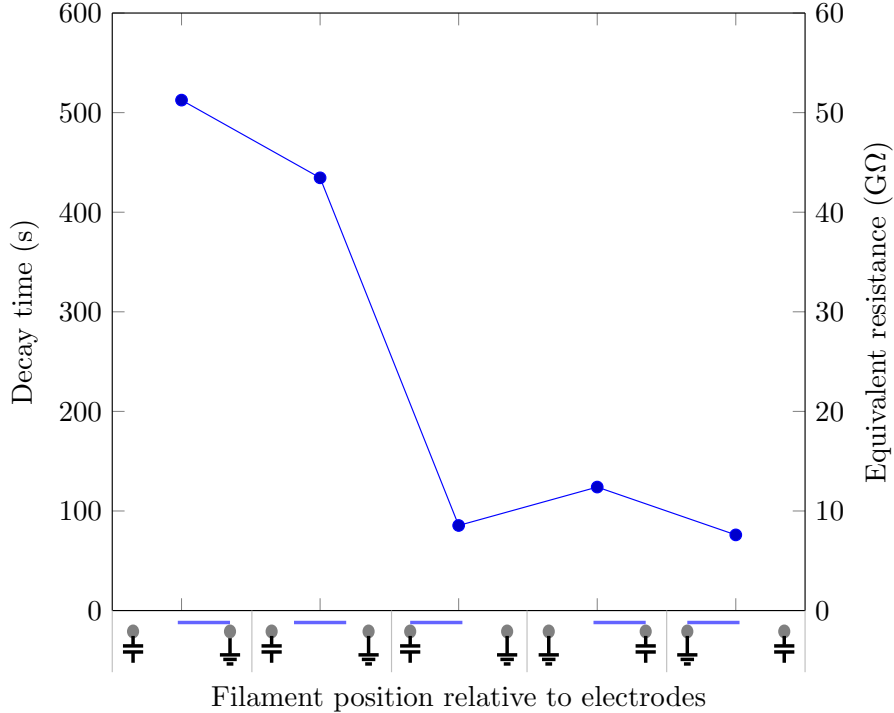


Figure 6: Charge decay time as a function of the relative position of the filament and the electrodes, located 2 mm away from the laser beam. On the symbols of the x -axis, the laser filament (in blue) propagates from left to right. The capacitor is charged at +14 kV and the gap between the electrodes is 40 cm.

Finally, we note that the unloading of a negative electrode facing a ground electrode behaves similar to that of a positive electrode *vs.* ground.

IV. DISCUSSION

As the filament offers a long conductor of 100 μm diameter similar to ultra-corona generating devices used to prevent sparking [28], it can be expected that its effect relies on a similar mechanism. Offering a sharp conducting surface, ultra-corona devices strongly deform and enhance the electric field locally. In the case of anode corona, the electrons are accelerated towards the electrode, leaving a space charge of positive ions behind them. Furthermore, they generate secondary charges by avalanche ionization in the air, as well as impact ionization on the electrode surface [28, 30, 31]. The local positive charge left behind by the electrons locally creates a strong electric field that in turn can field-ionize additional

air molecules further apart. The resulting charge flow is visible as a glow discharge and audible by naked ear. Furthermore the partial screening of the electric field drastically increases in the breakdown voltage, similar to the charge neutralization and the electrical arc suppression by the filaments.

However, filaments differ from a conducting wire in several ways. They generate a long, connected 100 μm diameter plasma with an electron density of at least $\rho_{\text{fil}} = 10^{21} \text{ m}^{-3}$ and a lifetime in the μs range [20, 21], seven orders beyond typical values in a corona, $\rho_c = 10^{14} \text{ m}^{-3}$ [32]. These electrons are free to spread around the laser beam, not being confined to the initial conducting volume. As a consequence, much more space charges can be generated over much larger volumes. Furthermore, during the electron lifetime, their displacement can strongly affect the electric field, and induce significant currents.

A rough estimate of this particular aspect can be obtained by considering the electron mobility [36]:

$$\mu_e(m^2/V \cdot s) = -\frac{N_0}{3N} \left(\frac{5 \times 10^5 + E_0}{1.9 \times 10^4 + 26.7 \times E_0} \right)^{0.6} \quad (1)$$

where $E_0 = EN_0/N$, E is the electric field, and N and N_0 are the molecule densities in the considered condition and in normal conditions, respectively.

As a result, if we neglect ionic mobility, the resistance of the plasma over a pathway L expresses as:

$$R = \frac{1}{e\mu_e S} \int_0^L \frac{d\vec{r}}{\rho_e(\vec{r})} \quad (2)$$

where S is the cross-section of the conducting area and ρ_e the free electron density.

According to Equation (1), $\mu_e = 0.2 \text{ m}^2/\text{V}\cdot\text{s}$ for an electric field of 50 kV/m, including electron drift speeds close to 10^4 m/s , corresponding to 10 cm within 1 μs , a typical plasma lifetime in the electric field [33]. We therefore expect a monotonic decay of the electron density for increasing distances r around the filament. Assuming an exponential decay, the electron density between the filament and the electrode, at a distance r from the filament, is modeled by $\rho_e(r) = \rho_{\text{fil}} \exp(-r \ln \rho/L)$, with $\rho = \rho_{\text{fil}}/\rho_c$. As a consequence,

$$R = \frac{L}{e\mu_e S \rho_{\text{fil}}} \frac{\rho - 1}{\ln \rho} \approx \frac{L}{e\mu_e S \rho_{\text{fil}}} \frac{\rho}{\ln \rho} \quad (3)$$

which amounts to 20 M Ω for a cross-section $S = 1 \text{ cm}^2$ typically corresponding to a column of air with a cross-section comparable to that of the electrodes, and a length $L = 10 \text{ cm}$.

However, the μs plasma lifetime [33] is much shorter than the ms time between two laser pulses at a repetition rate of 1000 Hz. This 1/1000 duty cycle will result in a 1000-fold higher effective resistance. Furthermore, the current measured in our experiment flows from the HV electrode to ground electrode, via the filament and the two gaps between the electrodes and the filament. Consequently, our crude estimate yields a value of 40 G Ω for the whole path when the filament is 10 cm away from the electrodes. This value matches well the experimental one (See Figure 5). We note that the resistance of the filament itself has been neglected, as it lies in the M Ω /m range [11], well below the gap between the filament and the electrodes.

Although the above discussion disregards the plasma dynamics, including the plasma lifetime and the avalanche, and it does not consider the contribution of the heavy species both to the field deformation and to the current flow, this estimation illustrates the critical contribution of the high electron densities generated in the filament on the electrical arc suppression by ultra-corona generation. It also explains why the two ends of the filament behave differently (Figure 6), related with the differences in their longitudinal electron density profiles.

Another specificity of the filament as compared to the wire-based ultra-corona generating devices is that the former is not grounded. Although it may be surprising that grounding is not necessary to generate ultra-corona, it is reminiscent of the triggering of lightning by rockets pulling only a short section of conducting wire, without connection to the ground. The local exaltation of the electric field is sufficient to initiate the discharge [34]. Furthermore, filaments provide a large amount of charge available to neutralize the high-voltage, not requiring supply from the ground.

More specifically, one can roughly estimate the amount of charge available for the neutralization, e.g., considering the conditions of Figure 4, where a 10 nF capacitor loaded under 10 kV is unloaded in typically 40 s. The 3–4 filaments of our setup neutralize $Q_0 = 10^{-4}$ C. In comparison, the charge produced in a 16 cm-long section of 100 μm diameter, with an electron density $\rho_{\text{fil}} = 10^{21} \text{ m}^{-3}$ in a single filament amounts to 200 nC. Over 40 s, the setup will therefore have produced 8 mC. This value lies two orders of magnitude beyond the initial charge to neutralize. It may even be underestimated as the electron density generated by the filaments could be higher.

V. CONCLUSION

As a conclusion, we have observed suppression of electrical arcs by laser filaments. This effect is efficient even remotely, up to distances at least twice the gap between the electrodes. Filaments generated by ultrashort laser pulses provide a $100\ \mu\text{m}$ thin conducting channel. Similar to metallic wires of comparable diameter producing ultra-corona [28], they locally enhance the electric field, releasing high concentrations of space charge that allow current to flow and neutralize the electrodes, reducing the electrode potential and preventing sparking.

This new phenomenon opens the way to new approaches to lightning and over-voltage protection. As compared with a metallic thin wire, filaments generated in the air are generated by each laser pulse and therefore avoid any problem of mechanical resistance.

ACKNOWLEDGMENTS

We acknowledge financial support from the ERC advanced grant "Filatmo". We thank I. Crasse, D. Eeltink, S. Hermelin, M. Matthews, and M. Moret for experimental assistance, and N. Berti for numerical support.

-
- [1] E. P. Krider, "Benjamin franklin and the first lightning conductors," *History of Meteorology* **1**, 1–13 (2004).
 - [2] C. Gary, "La foudre. Nature, histoire, risques et protection," (Dunod, Paris, 2004).
 - [3] M. Miki, Y. Aihara, and T. Shindo, "Development of long gap discharges guided by a pulsed CO₂ laser," *J. Phys. D : Applied physics* **26**, 1244–1252 (1993).
 - [4] X. M. Zhao, J.-C. Diels, C. Y. Wang, and J. M. Elizondo, "Femtosecond ultraviolet laser pulse induced lightning discharges in gases," *IEEE J. Quantum Electron.* **31**, 599–612 (1995).
 - [5] S. Uchida, Y. Shimada, H. Yasuda, S. Motokoshi, C. Yamanaka, T. Yamanaka, Z. Kawasaki, and K. Tsubakimoto, "Laser-triggered lightning in field experiments," *J. Opt. Technol.* **66**, 199–202 (1999).
 - [6] D. Comtois, C. Y. Chien, A. Desparois, F. Gérin, G. Jarry, T. W. Johnston, J. C. Kieffer, B. L. Fontaine, F. Martin, R. Mawassi, H. Pépin, F. A. M. Rizk, F. Vidal, P. Couture, H. P. Mercure,

- C. Potvin, A. Bondiou-Clergerie, and I. Gallimberti, “Triggering and guiding leader discharges using a plasma channel created by an ultrashort laser,” *Appl. Phys. Lett.* **76**, 819–821 (2000).
- [7] E. M. Bazelyan and Y. P. Raizer, “The mechanism of lightning attraction and the problem of lightning initiation by lasers,” *Physics - Uspekhi* **43**, 701 (2000).
- [8] B. La Fontaine, D. Comtois, C. Y. Chien, A. Desparois, F. Gérin, G. Jarry, T. W. Johnston, J. C. Kieffer, F. Martin, R. Mawassi, H. Pépin, F. A. M. Rizk, F. Vidal, C. Potvin, P. Couture, and H. P. Mercure, “Guiding large-scale spark discharges with ultrashort pulse laser filaments,” *J. Appl. Phys.* **88**, 610–615 (2000).
- [9] P. Rambo, J. Schwarz, and J.-C. Diels, “High-voltage electrical discharges induced by an ultrashort-pulse UV laser system,” *J. Opt. A: Pure Appl. Opt.* **3**, 146–158 (2001).
- [10] V. V. Apollonov, L. M. Vasilyak, I. P. Vereshchagin, V. V. Glazkov, D. N. Gerasimov, I. G. Kononov, A. V. Orlov, D. N. Polyakov, O. A. Sinkevich, M. V. Sokolova, A. G. Temnikov, and K. N. Firsov, “Experimental simulation of a laser lightning-protection system on a device with an artificial cloud of charged aqueous aerosol,” *Quantum Electron.* **32**, 523 (2002).
- [11] M. Rodriguez, R. Sauerbrey, H. Wille, L. Wöste, T. Fujii, Y.-B. André, A. Mysyrowicz, L. Klingbeil, K. Rethmeier, W. Kalkner, J. Kasparian, E. Salmon, J. Yu, and J.-P. Wolf, “Triggering and guiding megavolt discharges by use of laser-induced ionized filaments,” *Opt. Lett.* **27**, 772–774 (2002).
- [12] J. Kasparian, M. Rodriguez, G. Méjean, J. Yu, E. Salmon, H. Wille, R. Bourayou, S. Frey, Y.-B. André, A. Mysyrowicz, R. Sauerbrey, J.-P. Wolf, L. Wöste. “White-Light Filaments for Atmospheric Analysis,” *Science* **301**, 61-64 (2003).
- [13] J. Kasparian, R. Ackermann, Y.-B. André, G. Méchain, G. Méjean, B. Prade, P. Rohwetter, E. Salmon, K. Stelmaszczyk, J. Yu, A. Mysyrowicz, R. Sauerbrey, L. Wöste, and J.-P. Wolf, “Electric events synchronized with laser filaments in thunderclouds,” *Opt. Express* **16**, 5757–5763 (2008).
- [14] K. Sugiyama, T. Fujii, M. Miki, M. Yamaguchi, A. Zhidkov, E. Hotta, and K. Nemoto, “Laser-filament-induced corona discharges and remote measurements of electric fields,” *Opt. Lett.* **34**, 2964–2966 (2009).
- [15] K. Sugiyama, T. Fujii, M. Miki, A. Zhidkov, M. Yamaguchi, E. Hotta, and K. Nemoto, “Submicrosecond laser-filament-assisted corona bursts near a high-voltage electrode,” *Phys. Plasmas* (1994-present) **17**, 043108 (2010).

- [16] S. Eto, A. Zhidkov, Y. Oishi, M. Miki, and T. Fujii, “Quenching electron runaway in positive high-voltage-impulse discharges in air by laser filaments,” *Opt. Lett.* **37**, 1130–1132 (2012).
- [17] A. Schmitt-Sody, D. French, W. White, A. Lucero, W. P. Roach, V. Hasson. “The importance of corona generation and leader formation during laser filament guided discharges in air,” *Appl. Phys. Lett.* **106**, 124101 (2015).
- [18] Tie-Jun Wang, Yingxia Wei, Yaoxiang Liu, Na Chen, Yonghong Liu, Jingjing Ju, Haiyi Sun, Cheng Wang, Haihe Lu, Jiansheng Liu, See Leang Chin, Ruxin Li, and Zhizhan Xu “Direct observation of laser guided corona discharges,” arXiv:1508.03966 (2015)
- [19] S. L. Chin, S. A. Hosseini, W. Liu, Q. Luo, F. Théberge, N. Aközbek, A. Becker, V. P. Kandidov, O. G. Kosareva, and H. Schröder, “The propagation of powerful femtosecond laser pulses in optical media: physics, applications, and new challenges,” *Canadian J. Phys.* **83**, 863–905 (2005).
- [20] A. Couairon and A. Mysyrowicz, “Femtosecond filamentation in transparent media,” *Phys. Rep.* **441**, 47–189 (2007).
- [21] L. Bergé, S. Skupin, R. Nuter, J. Kasparian, and J.-P. Wolf, “Ultrashort filaments of light in weakly-ionized, optically-transparent media,” *Rep. Prog. Phys.* **70**, 1633–1713 (2007). ArXiv: physics/0612063.
- [22] P. Bédjot, J. Kasparian, S. Henin, V. Loriot, T. Vieillard, E. Hertz, O. Faucher, B. Lavorel, and J.-P. Wolf, “Higher-order kerr terms allow ionization-free filamentation in gases,” *Phys. Rev. Lett.* **104**, 103903 (2010).
- [23] P. Bédjot, E. Hertz, B. Lavorel, J. Kasparian, J. Wolf, and O. Faucher, “Transition from plasma- to Kerr-driven laser filamentation,” *Phys. Rev. Lett.* **106**, 243902 (2011).
- [24] P. Bédjot, E. Cormier, E. Hertz, B. Lavorel, J. Kasparian, J.-P. Wolf, O. Faucher. “High-Field Quantum Calculation Reveals Time-Dependent Negative Kerr Contribution,” *Phys. Rev. Lett.* **110**, 043902 (2013).
- [25] D. L. Weerawarne, X. Gao, A. L. Gaeta, B. Shim. “Higher-Order Nonlinearities Revisited and Their Effect on Harmonic Generation,” *Phys. Rev. Lett.* **114**, 093901 (2015).
- [26] J. Kasparian, R. Sauerbrey, and S. L. Chin, “The critical laser intensity of self-guided light filaments in air,” *Appl. Phys. B* **71**, 877–879 (2000).
- [27] A. Becker, N. Aközbek, K. Vijayalakshmi, E. Oral, C. M. Bowden, and S. L. Chin, “Intensity clamping and re-focusing of intense femtosecond laser pulses in nitrogen molecular gas,” *Appl.*

- Phys. B **73**, 287–290 (2001).
- [28] F. Rizk, “Analysis of Space Charge Generating Devices for Lightning Protection: Performance in Slow Varying Fields,” *IEEE Trans. Power Delivery* **25**, 1996–2006 (2010).
- [29] S. D. Pawar, P. Murugavel, and D. M. Lal, “Effect of relative humidity and sea level pressure on electrical conductivity of air over Indian Ocean,” *J. Geophys. Res. D: Atmospheres* **114**, D02205 (2009).
- [30] C. A. E. Uhlig, The ultra corona discharge, a new phenomenon occurring on thin wires, High voltage symposium, National Research Council of Canada, Ottawa, Canada (1956).
- [31] F. A. M. Fizek, G. N. Trinh, “High Voltage engineering,” CRC Press (2014).
- [32] J. Chen and J. H. Davidson, “Electron Density and Energy Distributions in the Positive DC Corona: Interpretation for Corona-Enhanced Chemical Reactions,” *Plasma Chem. Plasma Processing* **22**, 199–224 (2002).
- [33] S. Tzortzakis, B. Prade, M. Franco, and A. Mysyrowicz, “Time evolution of the plasma channel at the trail of a self-guided IR femtosecond laser pulse in air,” *Opt. Commun.* **181**, 123–127 (2000).
- [34] V. A. Rakov, M. A. Uman, and K. J. Rambo, “A review of ten years of triggered-lightning experiments at Camp Blanding, Florida,” *Atmos. Res.* **76**, 503–517 (2005).

ERRATUM

In the discussion of [35], we erroneously converted the 10^4 m/s drift speed of the electrons into a $1 \mu\text{s}$ transit time through the $L = 10$ cm gap between the filament and the electrodes. The correct transit time of $10 \mu\text{s}$ is well beyond the electron lifetime, preventing them to reach the electrode and ensure the conduction, at least in a streamer at a temperature close to ambient. As a consequence, their distribution cannot be modelled as an exponential decay between the filament and the electrodes, so that Eq. (3) is irrelevant and electrons cannot ensure the observed remote unloading under the experimental conditions of [35].

Rather, the ions have a mobility of $2 \times 10^{-4} \text{ m}^2/\text{Vs}$ [36], hence a drift speed 10 m/s under an electric field of 50 kV/m . Therefore, they transit in 10 ms . After that time, their concentration is still $2 \times 10^{19} \text{ m}^{-3}$ according to the plasma model described in [37]. This ion density is sufficient to ensure the observed conductivity of several tens of $\text{G}\Omega$ [35], a conclusion consistent with recent results on electric probing of filaments [38]. However, in the case of large electric fields leading to a leader-like regime [39], a contribution of the electrons along with the ions may still be considered.

Erratum references

- [35] E. Schubert, D. Mongin, J. Kasparian, J.-P. Wolf, “Remote electrical arc suppression by laser filamentation,” *Opt. Express* **23**, 28640 (2015)
- [36] X. M. Zhao, J.-C. Diels, C. Y. Wang, and J. M. Elizondo, “Femtosecond ultraviolet laser pulse induced lightning discharges in gases,” *IEEE J. Quant. Electron.* **31**, 599–612 (1995).
- [37] E. Schubert, J.-G. Brisset, M. Matthews, A. Courjaud, J. Kasparian, J.-P. Wolf. “Optimal laser-pulse energy partitioning for air ionization,” *Phys. Rev. A* **94**, 033824 (2016)
- [38] P. Polynkin, “Mobilities of O_2^+ and O_2^- ions in femtosecond laser filaments in air,” *Appl. Phys. Lett.* **101**, 164102 (2012)
- [39] T. Fujii, M. Miki, N. Goto, A. Zhidkov, T. Fukuchi, Y. Oishi, and K. Nemoto, “Leader effects on femtosecond-laser-filament-triggered discharges,” *Phys. Plasmas* **15**, 13107 (2008).